UC Irvine
UC Irvine Previously Published Works

Title

Structure and Function of Embryonic Rat Retinal Sheet Transplants

Permalink

https://escholarship.org/uc/item/8c95w3w7

Journal

Current Eye Research, 32(9)

ISSN

0271-3683

Authors

Peng, Qing
Thomas, Biju B
Aramant, Robert B
et al.

Publication Date

2007

DOI

10.1080/02713680701530597

Peer reviewed

informa
healthcare

Structure and Function of Embryonic Rat Retinal Sheet Transplants

Qing Peng
Department of Ophthalmology,
First Hospital of Shanxi Medical
University, Taiyuan, Shanxi,
People's Republic of China;
Ophthalmology-USC, Doheny
Eye Institute, Los Angeles,
California, USA

Biju B. Thomas
Ophthalmology-USC, Doheny
Eye Institute, Los Angeles,
California, USA

Robert B. Aramant
Anatomical Sciences &
Neurobiology, University of
Louisville, Louisville,
Kentucky, USA

**Zhenhai Chen
and Srinivas R. Sadda**
Ophthalmology-USC, Doheny
Eye Institute, Los Angeles,
California, USA

Magdalene J. Seiler
Ophthalmology-USC, Doheny
Eye Institute, Los Angeles,
California, USA; Cell &
Neurobiology-USC,
Los Angeles, California, USA; UC
California at Irvine, Department
of Anatomy and Neurobiology,
Irvine, California, USA

Correspondence: Dr. Biju B. Thomas,
Doheny Retina Institute, Doheny Eye
Institute, Keck School of Medicine,
University of Southern California,
1450 San Pablo Street, Los Angeles,
CA 90033, USA. E-mail:
bthomas@doheny.org

ABSTRACT *Purpose*: To evaluate retinal sheet transplants in S334ter-line-3 retinal degenerate rats by comparing visual responses recorded electrophysiologically with morphology based on light and electron microscopy. *Methods*: S334ter-line-3 retinal degenerate rats (n = 7) received retinal sheet transplants between postnatal days 28 and 31. The donor tissue was derived from transgenic embryonic day 19 (E19) rat retinae expressing human placental alkaline phosphatase (hPAP). Fresh retinal sheets were gently transplanted into the subretinal space of the left eye with the help of a custom-made implantation tool. Selected rats (n = 5) were subjected to electrophysiologic evaluation of visual responses from the superior colliculus about 84–121 days after surgery. Transplanted eyes were processed for light microscopy (LM) and electron microscopy (EM) evaluations. *Results*: All the transplanted rats that were evaluated for visual responses in the brain showed responses to very low light stimulation (-3.42 to -2.8 log cd/m^2) of the eye in a small area of the superior colliculus corresponding with the placement of the transplant in the host retina. Histologic evaluation showed that most of the transplants contained well-laminated areas with correct polarity in the subretinal space. Inside the transplant areas, rosettes of photoreceptors with inner and outer segments were found. In the laminated areas, the outer segments of photoreceptors were facing the host retinal pigment epithelium (RPE). Immunohistochemical evaluation of hPAP donor cells revealed areas with specific staining of the transplants in the subretinal space. Electron microscopic evaluation showed a glial demarcation membrane between the host and the transplant, however, processes originating from the transplant were observed inside the host retina. *Conclusions*: Sheets of E19 rat retina transplanted into the subretinal space of S334ter-line-3 rats survived without immune rejection and continued to show visual function when tested after 3 months. Well-developed photoreceptors and many synapse types were seen within the transplants. hPAP staining showed a certain degree of integration between the host retina and the transplant suggesting that transplanted photoreceptors contributed to the restored light sensitivity.

KEYWORDS human placental alkaline phosphatase; retinal degeneration; retinal transplantation; superior colliculus; ultrastructure

INTRODUCTION

Retinal degeneration is a leading cause of blindness in the Western world. Major diseases causing retinal degeneration are age-related macular degeneration (AMD) and retinitis pigmentosa (RP). Currently, different approaches are used to rescue or restore vision in humans. One major treatment strategy is cell replacement therapy, which consists of subretinal delivery of cell suspensions,[1−3] cell microaggregates,[4−8] and photoreceptor sheets[9−11] into the diseased eye. Intact sheets of fetal or neonatal retina have also been transplanted into degenerated eyes with the aim of restoring visual function.[12−15] Other treatment strategies include gene therapy,[16−18] visual prosthetics,[19−22] and pharmacotherapies.[23,24] Based on various functional tests performed in animal models, visual restoration has been reported after retinal sheet transplantation.[11,13,25−27] Initial encouraging results obtained from animal experiments persuaded researchers to perform retinal transplantation surgeries in human patients,[10,28−31] and some studies yielded promising results.[30]

Our group has been focused on transplanting sheets of fetal retina into the subretinal space using a special device that allows gentle placement of the fragile donor tissue as a flat sheet with the proper orientation/polarity. These sheets were shown to develop a normal lamination pattern in a variety of rat models of retinal degeneration[14,32,33] and restored visual responses in the superior colliculus (SC).[13,26,27,34,35] The mechanism of this visual restoration has not been well established, and a detailed ultrastructural evaluation of the extent of integration between the host and transplanted sheet has not been performed.

In the current investigation, the structural and functional characteristics of embryonic sheet transplants in S334ter-line-3 retinal degenerate rats were studied by light microscopy (LM) and electron microscopy (EM) combined with electrophysiologic evaluation of the visual responses from the superior colliculus (SC) of the brain.

MATERIALS AND METHODS

Animals

In this study, all animals were treated according to the NIH Guide for the Care and Use of Laboratory Animals, the ARVO Statement for the Use of Animals in Ophthalmic and Vision Research, and according to an approved protocol by the Doheny Eye Institute, University of Southern California IACUC.

S334ter-line-3 were produced by Xenogen Biosciences (formerly Chrysalis DNX Transgenic Sciences, Princeton, NJ, USA), and developed and supplied with the support of the National Eye Institute by Dr. Matthew LaVail, University of California San Francisco. The F1 generation of a cross between homozygous line-3 and pigmented Copenhagen rats (Harlan, Indianapolis, IN, USA) was used for the experiments. These rats with a mutated rhodopsin gene have an early retinal degeneration and develop no outer segments; only one to two rows of photoreceptors remain at postnatal days 28–30. Donor cells for this study were derived from transgenic rats expressing human alkaline phosphatase (hPAP) in the cytoplasm of all cells[36,37] that were bred with ACI rats (Harlan) to produce a pigmented strain.

Transplantation

Details of the transplantation surgery used in this study were described previously.[14,38] Briefly, donor retinal tissues were obtained from pigmented hPAP rat fetuses at E19 by caesarean section. The fetal retina was carefully dissected free from the surrounding tissues. A small piece with average size 0.5×1.2 mm^2 was prepared for transplantation. S334ter-3 rats were anesthetized by intraperitoneal injection of a mixture of ketamine 37.5 mg kg^{-1} and xylazine 5 mg kg^{-1}in sterile saline and their pupils dilated by topical application of 1% atropine sulfate. A small incision (approximately 1 mm) was cut behind the pars plana. A custom-made implantation tool (US Patent No. 6 159 218), loaded with a retinal sheet, was carefully placed into the subretinal space in the superior nasal quadrant of the host retina, and the donor tissue was released slowly and gently. The scleral incision was closed with 10-0 sutures. Immediately after the surgery, the fundus of the rat was examined by a contact lens on the cornea to identify the transplant placement.

Electrophysiology

Electrophysiologic assessment of visual responses in the SC was performed after the modified method described previously.[39] Briefly, the rats were dark-adapted overnight, and eyes were covered with a custom-made eye cap that prevented bleaching of the photoreceptors during surgery to expose the surface

of the SC. The eye cap could be easily removed at the time of visual stimulation. Animals were initially anesthetized by intraperitoneal injection of ketamine/xylazine (37.5 mg/kg ketamine and 5 mg/kg xylazine) and later by a gas inhalant anesthetic (1.0% to 2.0% halothane in 40% O_2/60% N_2O) administered via an anesthetic mask (Stoelting Company, Wood Dale, IL, USA). Multiunit visual responses were recorded extracellularly from the superficial laminae of the exposed SC using nail polish–coated tungsten microelectrodes. At each recording location, which covers the whole extent of the SC surface, up to 16 presentations of a full-field illumination (controlled by a camera shutter) were projected on a white Plexiglas screen placed 10 cm in front of the contralateral eye. The intensity of the light stimulus at the beginning of the recording was -6.46 log cd/m^2 and gradually increased (controlled by neutral-density filters) until the visual threshold was measured. An interstimulus interval of 6 s was used. All electrical activity was recorded using a digital data acquisition system (Powerlab; ADI Instruments, Mountain View, CA, USA) and responses (8–16 sweeps) at each SC site were averaged using MATLAB software (R2006b). Blank trials, in which the illumination of the eye was blocked with an opaque filter, were also recorded.

Histology

Rats were perfusion fixed with a mixture of 4% paraformaldehyde and 0.4% glutaraldehyde in 0.1 M sodium phosphate buffer solution. The eyes were enucleated and put into 4% paraformaldehyde and 0.1% glutaraldehyde in 0.1 M cacodylate buffer (PH 7.4). The anterior segment was then removed and the posterior eyecup was postfixed in the same fixative for 6 hr at room temperature. After washing the eyecups several times with 0.1 M sodium cacodylate buffer, small pieces of specimens containing the transplant were dissected and embedded in 4% agarose with correct orientation. Vibratome sections were cut at 80 μm. Sections with transplants were further processed for hPAP immunohistochemistry with DAB staining (ABC method).

Immunohistochemistry

Selected vibratome sections were washed five times for 10 min in 0.1 M phosphate buffer (PB) and then were incubated for one-half an hour in 1% sodium borohydride (NaBH$_4$) in 0.1 M PB. After washing sections five times for 10 min again, the sections were run through 10%, 25%, 40%, 25%, and 10% ethanol (7 min each) followed by three 10-min PB washes. Vibratome sections were washed with phosphate-buffered saline (PBS) and incubated for 2 hr in 20% horse serum. The sections were incubated with a mouse monoclonal antibody against hPAP-antigen (Sigma, St. Louis, MO, USA) at a dilution of 1:1 200 at 4°C. After 72 hr, the sections were incubated in a 1:200 dilution of Biotin-conjugated goat anti-mouse IgG (Chemicon, Temecula, CA, USA) for 18–24 hr at 4°C. After washing five times (10 min each) with PBS, the sections were incubated overnight at 4°C in Elite ABC conjugated to horseradish peroxidase (Vector Labs, Burlingame, CA, USA). After five 10-min washings with PBS, the sections were stained for peroxidase activity by preincubation in diaminobenzidine tetrahydrochloride (DAB) substrate kit without H_2O_2 (Vector Labs). After 30 min, the incubation medium was exchanged with fresh DAB solution containing 0.01% H_2O_2.[40] The DAB reaction was stopped at 5–7 min and five 10-min washing in PBS were followed in 0.05 M Tris-HCl buffers. Sections were observed by light microscopy, and better-stained sections were selected for electron microscopic processing. Other vibratome sections were processed for Epon embedding without immunohistochemistry.

Electron Microscopy

Sections were washed five times with 0.1 M cacodylate buffer (10 min each) and then postfixed for 1 hr in 3% glutaraldehyde in 0.1 M cacodylate buffer for 2 hr in 2% osmium tetroxide in cacodylate buffer at 4°C, dehydrated through graded ethanols, and embedded in Epon. Some sections were not postfixed and embedded in LR White Resin (EMS, Hatfield, PA, USA). Semithin sections (1 μm) were stained with toluidine blue for Epon sections or hematoxylin and eosin (H&E) for LR White Resin sections. Ultrathin sections approximately 70 nm thick were cut with a diamond knife and stained with uranyl acetate and lead citrate. Counterstaining was omitted for some pre-embedding immunosamples. Sections were viewed and photographed on a Zeiss EM10 electron microscope (Thornwood, NY, USA).

RESULTS
Electrophysiology

Five transplanted rats that had clear corneas and lenses were selected for electrophysiologic evaluation
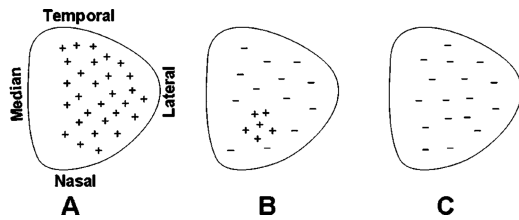
FIGURE 1 Schematic drawing representing the distribution of responses in the SC. (A) Normal pigmented rat, (B) S334ter-line-3 transgenic rat with retinal transplant, and (C) S334ter-line-3 transgenic rat without transplant. Plus signs indicate the presence of visual responses at a very low level of light stimulation, and minus signs indicate the absence of any visual response. In the S334ter-line-3 transgenic rat with retinal transplant, visual responses are found in the caudal SC area that represents the area in the retina corresponding with the placement of the graft.

Host Retina

The time course of photoreceptor degeneration was determined by examining the retinal morphology in S334ter-3 rats. Figure 3 shows retinal morphology in the normal rat, E19 rat, and S334ter-3 rat at different postnatal ages. Figure 3B shows the retinal morphology of E19 rat retina with ganglion cell layers; short inner plexiform layer (IPL) and the mostly undifferentiated neuroblastic outer retina (NBL). Figures 3C–3F demonstrate a progressive loss of outer segments over time. At postnatal day 11 (Fig. 2C), S334ter-3 retinas contained many degenerating rod photoreceptors with pyknotic nuclei in the outer nuclear layer (ONL). At postnatal day 18 (Fig. 3D), the ONL layers of S334ter-3 rats were obviously thinner than in normal rats with only 5–6 layers remaining. At P30 (Fig. 3E), only one row of photoreceptors remained, ONL and OPL were completely lost, and partially preserved inner nuclear layer (INL) directly faced the retinal pigment epithelium (RPE) in many areas. Rod photoreceptors are completely lost by postnatal day 45 (Fig. 3F).

of the visual responses from the SC. A schematic representation of the SC map showing the visual response areas in the transplanted rat is illustrated in Figure 1. Responses to very low light stimulation (-3.42 to $-2.8 \log cd/m^2$) could be recorded only from the SC of transplanted rats. These responses were recorded from an area of the SC corresponding with the placement of the transplant in the retina. Sample traces recorded from the superior colliculus of transplanted rats are shown in Figure 2. The responses recorded from the transplanted rats had comparatively longer latency and lower peak response amplitude than that of normal pigmented rats.
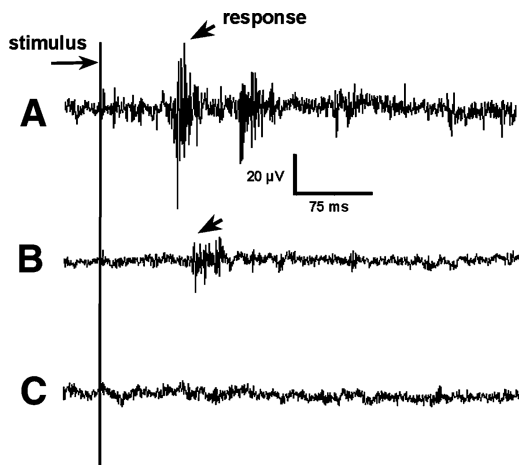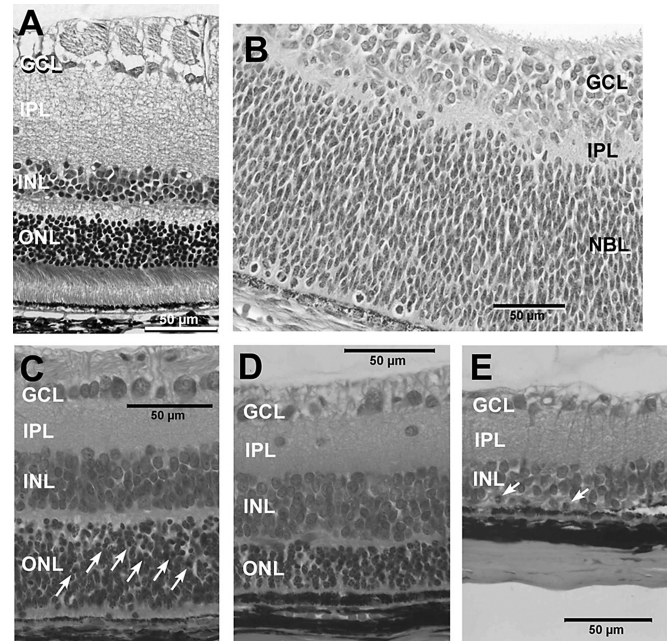

FIGURE 2 Traces of visual responses (average of 8–16 sweeps) to very low light stimulation (-3.42 to $-2.8 \log cd/m^2$) recorded from the superior colliculus. (A) Normal pigmented rats, (B) S334ter-line-3 retinal degenerate rats with retinal transplants, and (C) S334ter-line-3 retinal degenerate rats without retinal transplantation.

FIGURE 3 (A) Normal rat retina, Ganglion cell layer (GCL), inner plexiform layer (IPL), neuroblastic outer retina (NBL), outer nuclear layer (ONL), hematoxylin and eosin (H&E) Bar = 50 μm. (B) E19 rat retina. Bar = 50 μm. (C) S334ter-line-3 retina, postnatal day 11. Arrows indicate degenerating rod photoreceptors. Normal ONL, INL, IPL, and GCL. Bar = 50 μm. (D) Postnatal day 18. ONL reduced to 5–6 layers due to degeneration with normal INL, IPL, and GCL. H&E. Bar = 50 μm. (E) Postnatal day 30. Only INL, IPL, and GCL left. H&E. Bar = 50 μm.

Transplants

Semithin sections were stained with H&E and toluidine blue. Four transplants out of seven samples (57.1%) contained areas of laminated retina (about 20% to 30% of the transplant area) with parallel layers and fully developed photoreceptors with outer segments in contact with the host RPE (Fig. 4B). Few disorganized cells were found in the periphery of the transplant. Three transplants out of seven samples (42.9%) consisted largely of rosettes (Figs. 4A and 4C). The center of the rosettes contained the photoreceptors' outer segments with the ONL and INL around its periphery. The developing INL of the transplant was positioned adjacent to the remaining INL of host, and a relatively clear border between host and transplant could be seen (Figs. 4A and 4C). In the laminated transplants, photoreceptor inner and outer segments were observed with almost normal appearing retinal layers. The outer segments directly faced the host RPE with normally stacked disks. Well-developed outer nuclear layers of the transplants consisted of 8 to 10 rows of photoreceptor nuclei, but inner layers of transplant, in particular the inner nuclear layer, appeared to be less well developed (Figs. 4A and 4B). Outer segments were also observed inside rosettes, so that photoreceptors with outer segments could be found in more than 50% of the transplant area. The IPL of the transplant was in contact with the INL of the host with a distinct borderline between transplant and host (Fig. 4A). No inflammatory cells were observed in any of the samples.
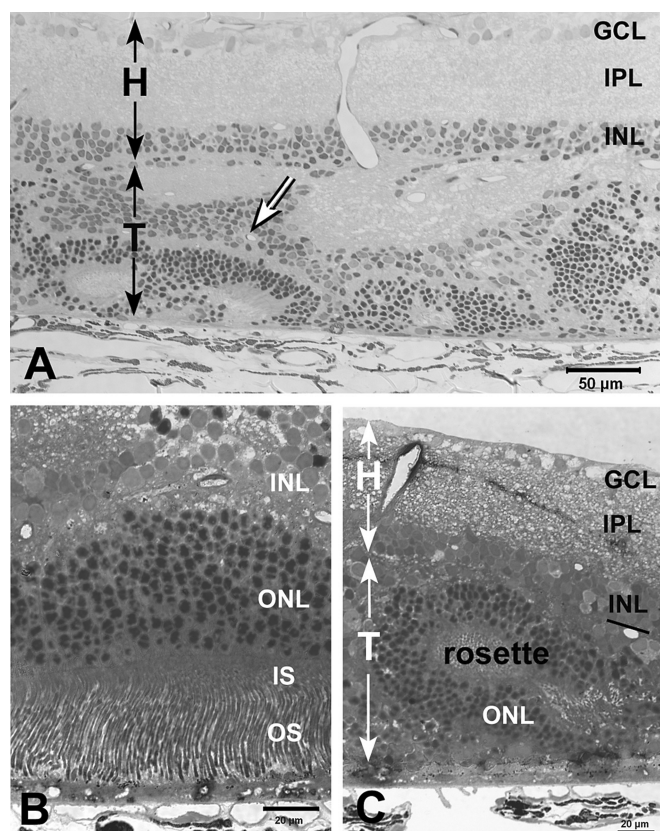

FIGURE 4 **(A)** Light micrograph of retinal transplant (T) in the subretinal space of S334ter rat (age 84 days, 60 days after surgery). Semithin section. Note edge of laminated area with parallel retinal layers with some photoreceptor outer segments (indicated by white arrow) transitioning into a rosette. Photoreceptors in other areas are disorganized. H&E. Bar = 50 μm. **(B)** Laminated area of transplant in subretinal space of S334ter-line rat (age 121 days, 90 days postsurgery). Transplant photoreceptors with outer segments in contact with host RPE. Host retina cannot be seen. Toluidine blue stain. Bar = 20 μm. **(C)** Transplant (T) in subretinal space of S334ter-line-3 rat host (H) (age 84 days, 60 days postsurgery). Photoreceptor rosettes. Toluidine blue stain. Bar = 20 μm.

Electron Microscopy

At day 60 postsurgery, relatively short transplant outer segments with a stacked disk configuration were observed that interdigitated with microvilli of the host RPE (Fig. 5A). The host RPE looked normal with phagosomes containing material from transplants outer segments, melanin granules, and other organelles. In the outer plexiform layers of the transplants, many well-developed photoreceptor terminals were seen that displayed the typical triad arrangement with characteristic synaptic ribbons and numerous invaginations with bipolar cell processes (Figs. 5B and 5C). Multisynaptic vesicles around ribbons were also observed in the transplant bipolar cells. In one specimen (Fig. 5D), an apparent synapse at the transplant-host interface, between the INL of the host and the IPL of the transplant, was observed. The transplant-host border was determined as being adjacent to the INL and the cone remnants of the host retina by zooming into the area from low to increasingly higher magnifications.

Immunohistochemistry for Donor Tissue (hPAP)

After hPAP immunohistochemistry with DAB staining of vibratome sections, well-laminated transplants were noticed with dark-brown staining showing the apparent border with the host retina (light-brown staining) (Fig. 6A). Some transplant processes penetrated the border into the INL of the host (Fig. 6B). Sections for ultrastructural analysis were taken from the area of border.
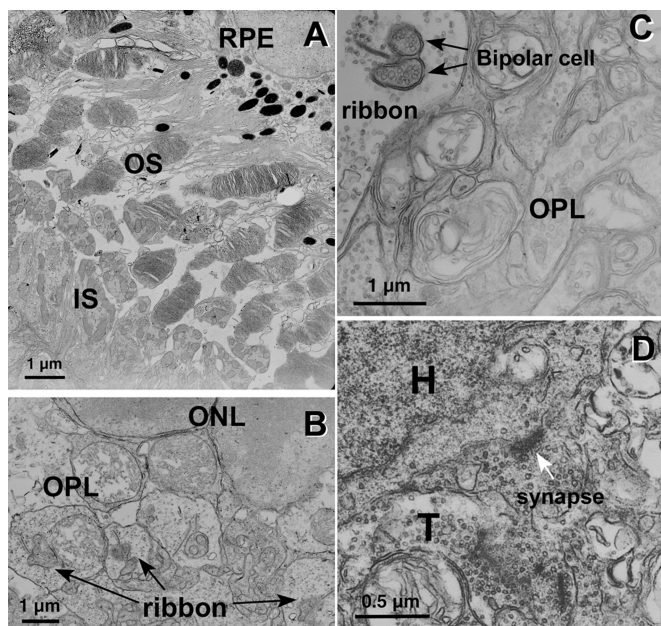
FIGURE 5 (A) Electron micrograph of transplant shown in Figure 4A. Short outer segments (OS), inner segments (IS), and outer nuclear layer (ONL). Bar = 1 μ m. (B) Photoreceptor terminals (ribbon synapses) in outer plexiform layer (OPL) of transplant shown in Figure 4B. Bar = 1 μm. (C) Enlargement of Figure 4B. A ribbon synapse in outer plexiform layer (OPL) of transplant. Bar = 1 μm. (D) Host (H) cell adjacent to inner plexiform layer of transplant (T). Apparent synapse between cell in host INL and bipolar cell in transplant IPL. Note many bipolar cell processes with synaptic vesicles. This section is at a deeper level of the vibratome slice, beyond the penetration of the antibody. The host-transplant border had been identified at a low magnification (not shown). Bar = 0.5 μm.

Ultrastructure After Immunohistochemistry

After identifying the border between host and transplant from the hPAP-stained vibratome slice, ultrathin sections were cut around these areas. Electron-dense DAB staining of the transplant showed an obvious border with the host retina. A glial demarcation membrane between host and transplant, which was derived from Muller cells processes, could be noticed clearly in some areas. However, processes originating from the transplant could often be observed inside the host retina. (Figs. 6C and 6D).

DISCUSSION
Restoration of Visual Responses

Electrophysiologic evaluation from the SC demonstrates that visual restoration occurs in S334ter-line-3 retinal degenerate rats that received fetal retinal sheet transplants. Previous investigations from our laboratory
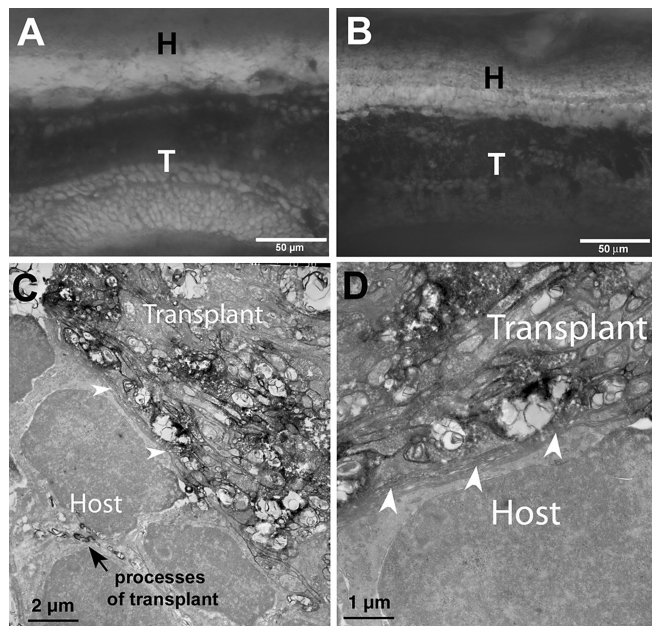

FIGURE 6 (A, B) hPAP-stained vibratome section. Transplant (T) is stained dark-brown. The host retina (H) is overall light brown. The inner and outer plexiform layers of the transplant are stained much darker than the nuclear layers. Bar = 50 μm. (C) Electron micrograph after pre-embedding immunohistochemistry for hPAP. Dark electron-dense staining of transplant inner plexiform layer. Note darkly stained transplant processes in the host (black arrow). Some apparent Muller cell processes filling the border between transplant and host (white arrow heads). Bar = 2 μm. (D) Enlargement of Fig. 6C. Muller cell processes filling in the border between host and transplant (white arrowheads). Bar = 1μm.

also demonstrated visual functional improvement in three different retinal degenerate rat models after retinal transplantation.[13,26,27,35] Although S334ter-line-3 rats were included in a previous study, the light stimulus consisted only of bright light (1300 cd/m^2), which could stimulate both host and transplant cones. The restorative effect of fetal retinal sheet transplants was reported to persist up to 100–150 days of age.[13] The current investigation attempted to correlate the functional results with the ultrastructural features of the transplant with the hope of gaining further insight into the mechanism of functional recovery.

The current investigation showed that the light sensitivity threshold in transplanted rats was in the mesopic range (-3.42 to -2.8 log cd/m^2). Because host rods should be absent, this observation suggests that transplant photoreceptors likely play a role in the functional restoration occurring after transplantation. Detailed morphologic evaluation based on EM studies was undertaken to confirm previous reports suggesting that the extent of functional recovery can be correlated with the morphologic quality of the transplants.[13,27,35]

A recent investigation performed in a mouse model suggested no correlation between functional data and the morphologic features of the transplant.[34] The discrepancies reported in the above studies indicate that the transplant effect depends on various extrinsic and intrinsic factors pertaining to the host environment. Two potential mechanisms may explain the functional recovery reported among transplanted rats. One mechanism is a direct replacement of degenerated photoreceptors with the transplanted photoreceptors establishing functional connections between the transplant and the host retina. This was suggested by preliminary histologic studies by our group.[14,15,41] Another mechanism is a humoral effect through the trophic factors released from the transplanted cells, especially rod photoreceptors,[42,43] which in turn may stimulate or facilitate the activity of the residual host photoreceptors.

Transplant Morphology

A detailed ultrastructural evaluation of the transplanted retina was undertaken to evaluate the extent of functional integration between the transplant and the host retina. SC recording data revealed that all transplanted rats were sensitive to very low level light stimulation and thus were good candidates to evaluate for the presence of features of integration. In this study, fetal retinal sheets were transplanted into the subretinal space using an instrument that maintains correct orientation/polarity. These results demonstrate that fetal retinal sheet transplants can develop parallel layers comparable with the normal retina with laminated areas of outer segments arranged parallel to the host RPE. Transplants survived up to 90 days postsurgery without any immune rejection. Many areas with normal appearing morphology and synaptic processes were apparent at the border between the transplant and the host retina. Some of these morphologic features were also reported from embryonic rabbit retinal transplants[44] and human retinal sheet transplants in rats,[45] however, no functional correlation was performed.

In the well-laminated transplants, the photoreceptor outer segments directly faced the RPE of the host; and the IPL of the transplant faced the INL of the host. Ultrastructural evaluation showed phagosomes inside the RPE of the host derived from the outer segment debris of transplant photoreceptors and demonstrated interactions between the transplant outer segments and host RPE cells. The presence of photoreceptor termi-nals (ribbon synapses and triad arrangements) could also be observed. In several areas inside the transplant, bipolar cell processes were also identified because of their distinctive invaginations at the photoreceptor terminals. Multiple synaptic vesicles were observed associated with many bipolar cell processes. The above morphologic features indicated that normal synapses had formed inside the transplant. Previous studies[14,44,45] showed well-developed photoreceptor terminals with horizontal and bipolar cell process invaginations in the outer plexiform layer, bipolar cell processes with many synapses in the inner plexiform layer, and processes with a lamellar pattern derived from Muller cells of the transplant filling in the border between transplant and host. Some apparent Muller cell processes were observed at the transplant-host border (Fig. 6D). Ghosh et al. inferred that these Muller cells possibly guided the neuron sprouting in the border.[46] In this border area, synapses of host cells with possible transplanted cells could be observed at 3 months postsurgery (example in Fig. 5D).

Morphologic evaluation of the transplant revealed that there were larger areas that developed into rosettes (i.e., photoreceptor outer segments in the center surrounded by ONL and other retinal layers). The formation of rosettes can have several causes. One major reason can be the presence of adherent junctions between the photoreceptors and the Muller cells at the outer limiting membrane, which is responsible for maintaining the intrinsic characteristics of the photoreceptor cells in a normal retina. The technical challenge of performing subretinal surgery in the small rat eye may contribute to rosette formation and disturbance of the underlying RPE, particularly if the instrument is placed at the wrong angle or pressure is exerted on the tissue during the time surgery.[14,47] Rosette formation routinely occurs after the transplantation of retinal microaggregates.[6,48,49]

Thus far, few studies have shown clear staining of the labeled retinal transplant cells and processes ultrastructurally. For example, retinal microaggregates of transgenic mice expressing the label lacZ in photoreceptors were transplanted to normal and rd mice.[6,50] Many transplantation studies have used GFP-labeled donor tissue.[34,51–53] Our study used hPAP-transgenic rats[37] as the donor. This made it relatively easy to identify the interface between the host and transplant thus enabling evaluation of morphologic integration.

In summary, sheets of E19 rat retina transplanted into the subretinal space of S334ter-line-3 rats survived

without immediate rejection and continued to show visual function when tested after 3 months. Ultrastructurally, well-developed photoreceptors and many normal synapse types were seen within the transplants. The border between the host and transplant could be clearly identified by hPAP immunohistochemistry, and a certain degree of integration between the host retina and the transplant was found suggesting that the transplanted photoreceptors may have contributed to the restored light sensitivity.

REFERENCES

[1] Algvere PV, Berglin L, Gouras P, Sheng Y, Kopp ED. Transplantation of RPE in age-related macular degeneration: observations in disciform lesions and dry RPE atrophy. *Graefes Archi Clin Exp Ophthalmol*. 1997;235:149–158.

[2] Juliusson B, Bergström A, van Veen T, Ehinger B. Cellular organization in retinal transplants using cell suspensions or fragments of embryonic retinal tissue. *Cell Transplant*. 1993;2:411–418.

[3] Li L, Turner JE. Optimal conditions for long-term photoreceptor cell rescue in RCS rats: the necessity for healthy RPE transplants. *Exp Eye Res*. 1991;52:669–679.

[4] Aramant RB, Seiler MJ, Ehinger B, Bergström A, Adolph AR, Turner JE. Neuronal markers in rat retinal grafts. *Dev. Brain Res.* 1990;53:47–61.

[5] Del Cerro M, Ison JR, Bowen GP, Lazar E, Del Cerro C. Intraretinal grafting restores function in light-blinded rats. *NeuroReport*. 1991;2:529–532.

[6] Gouras P, Du J, Kjeldbye H, Yamamoto S, Zack DJ. Long-term photoreceptor transplants in dystrophic and normal mouse retina. *Invest Ophthalmol Vis Sci.* 1994;35:3145–3153.

[7] Kwan AS, Wang S, Lund RD. Photoreceptor layer reconstruction in a rodent model of retinal degeneration. *Exp Neurol*. 1999;159:21–33.

[8] Seiler M, Aramant R. Transplantation of embryonic retinal donor cells labelled with BrdU or carrying a genetic marker to adult retina. *Exp Brain Res.* 1995;105:59–66.

[9] Berger AS, Tezel TH, Del Priore LV, Kaplan HJ. Photoreceptor transplantation in retinitis pigmentosa: short-term follow-up. *Ophthalmology*. 2003;110:383–391.

[10] Kaplan HJ, Tezel TH, Berger AS, Wolf ML, Del Priore LV. Human photoreceptor transplantation in retinitis pigmentosa. A safety study. *Arch Ophthalmol*. 1997;115:1168–1172.

[11] Silverman MS, Hughes SE, Valentino T, Liu Y. Photoreceptor transplantation: Anatomic, electrophysiologic, and behavioral evidence for the functional reconstruction of retinas lacking photoreceptors. *Exp Neurol.* 1992;115:87–94.

[12] Ghosh F, Wong F, Johansson K, Bruun A, Petters RM. Transplantation of full-thickness retina in the rhodopsin transgenic pig. *Retina*. 2004;24:98–109.

[13] Sagdullaev BT, Aramant RB, Seiler MJ, Woch G, McCall MA. Retinal transplantation-induced recovery of retinotectal visual function in a rodent model of retinitis pigmentosa. *Invest Ophthalmol Vis Sci*. 2003;44:1686–1695.

[14] Seiler MJ, Aramant RB. Intact sheets of fetal retina transplanted to restore damaged rat retinas. *Invest Ophthalmol Vis Sci*. 1998;39:2121–2131.

[15] Seiler MJ, Aramant RB. Transplantation of neuroblastic progenitor cells as a sheet preserves and restores retinal function. *Semin Ophthalmol*. 2005;20:31–42.

[16] Ali RR. Prospects for gene therapy. *Novartis Found Symp*. 2004;255:165–72; discussion 173–178.

[17] Dejneka NS, Rex TS, Bennett J. Gene therapy and animal models for retinal disease. *Dev Ophthalmol*. 2003;37:188–198.

[18] Delyfer MN, Leveillard T, Mohand-Said S, Hicks D, Picaud S, Sahel JA. Inherited retinal degenerations: therapeutic prospects. *Biol Cell*. 2004;96:261–269.

[19] Loewenstein JI, Montezuma SR, Rizzo JF, 3rd Outer retinal degeneration: an electronic retinal prosthesis as a treatment strategy. *Arch Ophthalmol*. 2004;122:587–596.

[20] Margalit E, Maia M, Weiland JD, et al. Retinal prosthesis for the blind. *Surv Ophthalmol*. 2002;47:335–356.

[21] Rizzo JF, 3rd, Wyatt J, Humayun M, et al. Retinal prosthesis: an encouraging first decade with major challenges ahead. *Ophthalmology*. 2001;108:13–14.

[22] Weiland JD, Liu W, Humayun MS. Retinal prosthesis. *Annu Rev Biomed Eng*. 2005;7:361–401.

[23] Caffe AR, Soderpalm AK, Holmqvist I, van Veen T. A combination of CNTF and BDNF rescues rd photoreceptors but changes rod differentiation in the presence of RPE in retinal explants. *Invest Ophthalmol Vis Sci*. 2001;42:275–282.

[24] Chong NH, Bird AC. Management of inherited outer retinal dystrophies: present and future. *Br J Ophthalmol*. 1999;83:120–122.

[25] Sauvé Y, Girman SV, Wang S, Lawrence JM, Lund RD. Progressive visual sensitivity loss in the Royal College of Surgeons rat: perimetric study in the superior colliculus. *Neuroscience*. 2001;103:51–63.

[26] Thomas BB, Aramant RB, Sadda SR, Seiler MJ. Retinal transplantation - a treatment strategy for retinal degenerative diseases. In: Hollyfield JG, Anderson RE, LaVail MM, *Retinal Degenerative Diseases*. New York: Springer: 2006:367–376.

[27] Thomas BB, Seiler MJ, Sadda SR, Aramant RB. Superior colliculus responses to light - preserved by transplantation in a slow degeneration rat model. *Exp Eye Res*. 2004;79:29–39.

[28] Algvere PV, Gouras P, Dafgard Kopp E. Long-term outcome of RPE allografts in non-immunosuppressed patients with AMD. *Eur J Ophthalmol*. 1999;9:217–230.

[29] Das T, del Cerro M, Jalali S, et al.. The transplantation of human fetal neuroretinal cells in advanced retinitis pigmentosa patients: results of a long-term safety study. *Exp Neurol*. 1999;157:58–68.

[30] Radtke ND, Aramant RB, Seiler MJ, Petry HM, Pidwell DJ. Vision change after sheet transplant of fetal retina with RPE to a retinitis pigmentosa patient. *Arch Ophthalmol*. 2004;122:1159–1165.

[31] Radtke ND, Seiler MJ, Aramant RB, Petry HM, Pidwell DJ. Transplantation of intact sheets of fetal neural retina with its retinal pigment epithelium in retinitis pigmentosa patients. *Am J Ophthalmol*. 2002;133:544–550.

[32] Aramant RB, Seiler MJ, Ball SL. Successful cotransplantation of intact sheets of fetal retinal pigment epithelium with retina. *Invest Ophthalmol Vis Sci*. 1999;40:1557–1564.

[33] Seiler MJ, Aramant RB, Ball SL. Photoreceptor function of retinal transplants implicated by light-dark shift of S-antigen and rod transducin. *Vision Res*. 1999;39:2589–2596.

[34] Arai S, Thomas BB, Seiler MJ, et al. Restoration of visual responses following transplantation of intact retinal sheets in rd mice. *Exp Eye Res*. 2004;79:331–341.

[35] Woch G, Aramant RB, Seiler MJ, Sagdullaev BT, McCall MA. Retinal transplants restore visually evoked responses in rats with photoreceptor degeneration. *Invest Ophthalmol Vis Sci*. 2001;42:1669–1676.

[36] Kisseberth WC, Brettingen NT, Lohse JK, Sandgren EP. Ubiquitous expression of marker transgenes in mice and rats. *Dev Biol*. 1999;214:128–138.

[37] Mujtaba T, Han SS, Fischer I, Sandgren EP, Rao MS. Stable expression of the alkaline phosphatase marker gene by neural cells in culture and after transplantation into the CNS using cells derived from a transgenic rat. *Exp Neurol*. 2002;174:48–57.

[38] Aramant RB, Seiler MJ. Retinal transplantation - advantages of intact fetal sheets. *Prog Retin Eye Res*. 2002a;21:57–73.

[39] Thomas BB, Aramant RB, Sadda SR, Seiler MJ. Light response differences in the superior colliculus of albino and pigmented rats. *Neurosci Lett*. 2005;385:143–147.

[40] Eldred WD, Zucker C, Karten HJ, Yazulla S. Comparison of fixation and penetration enhancement techniques for use in ultrastructural immunocytochemistry. *J Histochem Cytochem*. 1983;31:285–292.

[41] Seiler MJ, Sagdullaev BT, Woch G, Thomas BB, Aramant RB. Transsynaptic virus tracing from host brain to subretinal transplants. *Eur J Neurosci*. 2005;21:161–172.

[42] Fintz AC, Audo I, Hicks D, Mohand-Said S, Leveillard T, Sahel J. Partial characterization of retina-derived cone neuroprotection in two culture models of photoreceptor degeneration. *Invest Ophthalmol Vis Sci*. 2003;44:818–825.

[43] Mohand-Said S, Hicks D, Dreyfus H, Sahel JA. Selective transplantation of rods delays cone loss in a retinitis pigmentosa model. *Arch Ophthalmol*. 2000;118:807–811.

[44] Ghosh F, Bruun A, Ehinger B. Graft-host connections in long-term full-thickness embryonic rabbit retinal transplants. *Invest Ophthalmol Vis Sci*. 1999a;40:126–132.

[45] Aramant RB, Seiler MJ. Transplanted sheets of human retina and retinal pigment epithelium develop normally in nude rats. *Exp Eye Res*. 2002b;75:115–125.

[46] Ghosh F, Johansson K, Ehinger B. Long-term full-thickness embryonic rabbit retinal transplants. *Invest Ophthalmol Vis Sci*. 1999b;40:133–142.

[47] Aramant RB, Seiler MJ. Progress in retinal sheet transplantation. *Prog Retin Eye Res*. 2004;23:475–494.

[48] Aramant RB, Seiler MJ. Human embryonic retinal cell transplants in athymic immunodeficient rat hosts. *Cell Transplant*. 1994;3:461–474.

[49] Ehinger B, Bergström A, Seiler M, et al. Ultrastructure of human retinal cell transplants with long survival times in rats. *Exp. Eye Res.* 1991;53:447–460.

[50] Gouras P, Tanabe T. Survival and integration of neural retinal transplants in rd mice. *Graefes Arch Clin Exp Ophthalmol*. 2003;241:403–409.

[51] Guo Y, Saloupis P, Shaw SJ, Rickman DW. Engraftment of adult neural progenitor cells transplanted to rat retina injured by transient ischemia. *Invest Ophthalmol Vis Sci*. 2003;44:3194–3201.

[52] Lai CC, Gouras P, Doi K, et al. Tracking RPE transplants labeled by retroviral gene transfer with green fluorescent protein. *Invest Ophthalmol Vis Sci*. 1999;40:2141–2146.

[53] Mizumoto H, Mizumoto K, Shatos MA, Klassen H, Young MJ. Retinal transplantation of neural progenitor cells derived from the brain of GFP transgenic mice. *Vision Res*. 2003;43:1699–1708.

Embryonic Rat Retinal Sheet Transplants